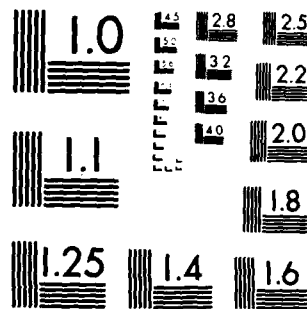


AD-A121 693 EFFICIENT ELASTIC-PLASTIC DESIGN OF SMALL FOUNDATIONS 171
(U) NAVAL RESEARCH LAB WASHINGTON DC G J O'HARA ET AL.
22 SEP 82 NRL-MR-4918 SBI-AD-E000 508

UNCLASSIFIED

F/G 13/13 NL

END
DATA
FILED
11-83
DTIC



MICROCOPY RESOLUTION TEST CHART
NATIONAL BUREAU OF STANDARDS-1963-A

3
NRL Memorandum Report 4710

AD A121653

Different Elastic-Plastic Design of Small Foundations

GEORGE J. O'HARA AND PATRICK F. CUNIFF

*Structural Integrity Branch
Marine Technology Division*

September 22, 1982

DTIC
ELECTED
NOV 22 1982

B

32 11 10 082

SECURITY CLASSIFICATION OF THIS PAGE (When Data Entered)

REPORT DOCUMENTATION PAGE		READ INSTRUCTIONS BEFORE COMPLETING FORM
1 REPORT NUMBER NRL Memorandum Report 4918	2 GOVT ACCESSION NO PP-P-1 673	3 RECIPIENT'S CATALOG NUMBER
4 TITLE (and Subtitle) EFFICIENT ELASTIC-PLASTIC DESIGN OF SMALL FOUNDATIONS		5 TYPE OF REPORT & PERIOD COVERED Interim report on a continuing NRL problem
		6 PERFORMING ORG REPORT NUMBER
7 AUTHOR(s) George J. O'Hara and Patrick F. Cunniff		8 CONTRACT OR GRANT NUMBER(S)
9 PERFORMING ORGANIZATION NAME AND ADDRESS Naval Research Laboratory Washington, DC 20375		10 PROGRAM ELEMENT PROJECT, TASK AREA & WORK UNIT NUMBERS SF 43-400-001 DTNSRDC 23102 58-1345-00
11 CONTROLLING OFFICE NAME AND ADDRESS		12 REPORT DATE September 22, 1982
		13 NUMBER OF PAGES 29
14 MONITORING AGENCY NAME & ADDRESS (if different from Controlling Office)		15 SECURITY CLASS (of this report) UNCLASSIFIED
		15a DECLASSIFICATION DOWNGRADING SCHEDULE
16 DISTRIBUTION STATEMENT (of this Report) Approved for public release; distribution unlimited.		
17 DISTRIBUTION STATEMENT (of the abstract entered in Block 20, if different from Report)		
18 SUPPLEMENTARY NOTES		
19 KEY WORDS (Continue on reverse side if necessary and identify by block number) Foundation design Shipboard shock Dynamic design		
20 ABSTRACT (Continue on reverse side if necessary and identify by block number) An elastic-plastic design analysis method is presented for small foundations which utilizes an energy criterion to insure against large deflections or unwanted collapse. The interaction effects from direct loads and shears are included, which has the effect of predicting a carrying capacity somewhat less than that of ordinary limit analysis. The energy storage capacity is calculated in a fashion which is conservative since the reduction of the planar moments of inertia is ignored. Several examples are worked out which use various beam like structures to illustrate the (Continued)		

DD FORM 1 JAN 73 1473 EDITION OF 1 NOV 69 IS OBSOLETE
S/N 0102-014-6601

SECURITY CLASSIFICATION OF THIS PAGE (When Data Entered)

SECURITY CLASSIFICATION OF THIS PAGE (When Data Entered)

20 ABSTRACT (Continued)

enhancement of carrying capacity from the sections contribution and of the indeterminate structural reactions. The results are worked up in detail, both theoretically and by numerical examples to show the ease of application and efficiency of this method.

S DTIC
ELECTE
NOV 22 1982 D

B



Accession For	
DTIS GRAIL	<input checked="" type="checkbox"/>
DTIC TAB	<input type="checkbox"/>
Announced	<input type="checkbox"/>
Classification	
By _____	
Distribution/	
Availability Codes	
Dist	Avail and/or Special
A	

SECURITY CLASSIFICATION OF THIS PAGE (When Data Entered)

CONTENTS

INTRODUCTION	1
ENVIRONMENTAL DESCRIPTION	1
LIMIT ANALYSIS	2
A Bending Effects	2
B Propped Cantilever Beam	2
STRESS RESULTANT THEORY	2
DESIGN CRITERIA	3
EXAMPLE PROBLEM	4
A Foundation Description	4
B Energy Storage Capacity	4
DESIGN REQUIREMENTS	6
A Equivalent Static Design	6
B Energy Design	6
Bending Energy Only	6
Bending and Shear Energy	6
C Effective Design Velocities, V_e	6
D Efficiency Factor	7
RESULTS	7
SUMMARY	9
REFERENCES	10
APPENDIX A - Limit Analysis of a Propped Cantilever Beam	11
APPENDIX B - Elastic-Plastic Interaction Effects	13
APPENDIX C - Reduced Moment of Inertia	14

EFFICIENT ELASTIC-PLASTIC DESIGN OF SMALL FOUNDATIONS

INTRODUCTION

An energy method has been reported earlier [1] that describes an efficient elastic design method for small foundations on shipboard structures. This method may be used to circumvent the Navy's Dynamic Design Analysis Method (DDAM) in those cases where a single degree of freedom (SDOF) system represents the equipment foundation structure. The assumption of a SDOF system is equivalent to saying that the static and dynamic stress and deflection patterns are the same so that a direct approach taking advantage of this can lead to an efficient design method that utilizes energy criteria.

The purpose of this report is to extend the energy method so that the foundation material undergoes elastic-plastic behavior. This new elastic-plastic energy method utilizes both limit analysis and the interaction effects between bending and shear as developed in plasticity theory. It is shown through an example problem that the method provides foundation designs that can lead to substantial weight and cost reductions.

For purposes of this report and its sample calculations the design is based upon the following hypothetical description of the shock environment. The equipment-foundation system shall be designed to withstand elasto-plastically the level of a 250-g equivalent static acceleration or a shock spectrum pseudo-velocity, V_g , of 8 ft/sec. The structure shall not experience a collapse mechanism so that all deflections remain small.¹

ENVIRONMENTAL DESCRIPTION

One of the vexing problems with DDAM has been the need to interpret measured shock response for purposes of developing design shock spectra. A significant contribution to this problem has been reported earlier [2]. It was shown that when equipment-foundation combinations yield under a shock input, the design shock spectra obtained is greater than the elastic design shock spectra.

To demonstrate this concept, consider Fig. 1 which shows an equipment that is attached to a vehicle by a foundation. This equipment-foundation structure is subjected to some shock input. Imagine that five foundations, identical except for their yield points, are to be each inverted and the combination is subjected to the same shock source. Since each has the same weight and some fixed base frequency, the elastic shock design value is the same in each case [3]. Also, assume that if the structure remained elastic, a 90 ksi stress would occur in the foundation.

The results might appear as in Fig. 2. This shows the shock design value versus fixed base frequency. Note that when the foundation was made of 30, 50, or 80 kw material, the apparent shock design values are greater than when it is either 100 or 150 ksi. Therefore, the elastic design value is a minimum so that the two high strength foundations remained elastic (maximum stress of 90 ksi), and the other three foundations went plastic. Thus, the weaker foundations give higher values for an elastic design. In other words, if a system were built of 100 ksi steel on the basis of the 50 kw steel test, the foundation would be overdesigned.

LIMIT ANALYSIS

A. Bending Effects

By way of introduction to limit analysis, consider the case of perfectly plastic behavior of a material by examining the stress distribution across a beam cross-section due to bending only as shown in Fig. 3. Figure 3(a) shows the elastic stress distribution where Mises's law holds and the tensile and compressive yield stresses are equal to each other. Figure 3(b) shows the elastic-plastic stress distribution as the applied load to the beam is increased. Here, the outer portions of the beam fibers have reached the elastic limit while the inner core of the beam remains elastic. Finally, as the load is increased further, the stress distribution reaches the fully plastic condition shown in Fig. 3(c). In this condition a plastic hinge is assumed to exist at the cross-section and the loads that just produce this condition are called the collapse loads.

Consider the cantilever beam with a rectangular cross-section subjected to the concentrated load P as shown in Fig. 4(a). The plastic hinge will form at the root of the beam where the maximum bending stresses occur. The load deflection relationship for this condition has been developed for the case of perfectly plastic behavior [4] and is sketched in Fig. 4(b). We observe that the collapse load P_c is 1.5 times greater than the elastic basic load P_0 . The corresponding deflection when the collapse mechanism is just reached is 2.22 times the elastic basic deflection δ_0 . The increase in the load P in going from the elastic basic to fully plastic behavior is denoted as the load enhancement, while the area under the load-deflection curve AB represents the energy enhancement as shown in Fig. 4(b). Of course, in an actual design we wish to stop short of reaching the collapse load. For a design method that utilizes energy, one approach for a conservative estimate of the energy enhancement would be to calculate the area under the curve AC. In effect we would be assuming that the beam remains elastic up to the collapse load. In reality, the beam behavior has been extended into the elasto-plastic region but short of reaching the collapse mechanism.

As a final comment on Fig. 4, it is noted that if the energy absorbed by the cantilever beam exceeds the area under the load-deflection curve (DAB), the design is an overdesign leading to the beam collapse criteria.

In addition to the cantilever beam in Fig. 4, other examples of beams subjected to a variety of loading conditions indicate that deflections due to bending moment increases could be on the order of four to five times the elastic basic deflections just near the collapse load. Consequently, if a procedure can guarantee that the collapse mechanism is not fully developed, then a design would be valid and weight and cost reductions would follow.

B. Propped Cantilever Beam

A second factor that contributes to load enhancement is to design the beam as a kinematically indeterminate structure. This leads us to consider the propped cantilever beam in Fig. 5 that carries two concentrated forces both of magnitude P . It is not readily apparent where the plastic hinges occur in order to carry out a limit analysis of the beam. A complete analysis is found in Appendix A which provides the correct plastic hinges that are shown in Fig. 6. The corresponding loading diagram, shear diagram, and bending-moment diagrams for this condition are shown in Figs. 7(a), 7(b), and 7(c) respectively, which we shall examine in greater detail in the example problem.

STRESS RESULTANT THEORY

The formation of the plastic hinges for the propped cantilever beam in Fig. 6 was based upon the effect of bending only. In reality, there is both shear and bending present throughout the beam as shown in Fig. 7. Shear effects become especially important for short deep beams and should not be

overlooked in the analysis. To account for the presence of both the shear force and bending moment at the highly stressed sections of the beam, the following interaction expression, that is developed in Appendix B, is applicable:

$$\left| \frac{M}{M_s} \right|^2 + \left| \frac{S}{S_s} \right|^2 = 1 \quad (1)$$

where M = bending moment present
 S = shear force present
 M_s = bending value of the bending modulus at the ultimate of shear
 S_s = bending value of the shear in the ultimate of bending.

This equation, therefore, will determine the validity category of the beam as demonstrated in the chart problem.

DESIGN CRITERIA

Consider the 90000 system illustrated as a beam as shown in Fig. 6. Let w be the weight of the equipment and an unguided problem of the foundation energy. The foundation needs to withstand the lower of 230 g or a pseudo velocity $\dot{x} = \Delta x / t = 0$ where Δx = relative displacement between the weight and the base.

The 170 g weight value is referred to weight factor and is shown in the example problem.

In the case of the velocity input, the kinetic energy of the 90000 system represents the energy absorbed by the foundation which is labelled E_r . If E_r is the energy storage capacity of the foundation then the required criteria for the equipment foundation connections is as follows:

$$E_r < E \quad (2)$$

That is, if the stored energy stored in the foundation is less than or equal to the energy storage capacity of the foundation, the structure will sustain the foundation effect. It is important that no energy is stored in the equipment.

Suppose the foundation consists of a base slab connected to a combination of bending, shear and direct load load. The energy absorbed by the beam for each type of load is represented as follows:

$$\text{Bending Energy} = E_b = \int_0^L \frac{M^2}{EI} dx \quad (3)$$

$$\text{Shear Energy} = E_s = \int_0^L \frac{S^2}{Gc} dx \quad (4)$$

$$\text{Direct Energy} = E_d = \int_0^L \frac{P^2}{2EI} dx \quad (5)$$

where M = bending modulus, S = shear, P = axial force, I = moment of inertia, E = cross-sectional area, G = shear modulus, c = span of I to the next area and L = length of the beam. The total available storage energy is

$$E_r = E_b + E_s + E_d \quad (6)$$

In the example problem developed in this report, only bending and shear will be present so that

$$E_r = E_b + E_s \quad (7)$$

It is also noted that Eq. (4) provides shear energy that closely follows a theory illustrated by Timoshenko [3].

The calculation for the bending energy represented by Eq. 13 does not take into account the reduced moment of inertia, I , that exists in the beam as discussed in Appendix C-1.

$$\int_1^L \frac{M^2}{2EI} < \int_1^L \frac{M^2}{2EJ} \quad (14)$$

where $J < I$. Furthermore by setting $\alpha = 1$ in Eq. 14 we shall obtain a situation where there is no

$$\int_1^L \frac{M^2}{2EI} < \int_1^L \frac{M^2}{2EJ} \quad (15)$$

consequently the increased stiffness provided by changing from a rectangular cross section to one that is available and has the same dimensions as the cross-sectional area.

EXAMPLE PROBLEM 20

C. Foundation Design

Consider the two proposed foundation designs in Fig. 2 that form the foundation for a rigidly attached piece of equipment. Both bases are 100 mm \times 75 rectangular foundation and it is assumed that they equally share the load in vertical shear. The foundation is rated with a tensile and compressive yield point of 70 kN and a shear yield point of 27 kN. The problem is to find the capacity capacity of these bases for the three environments described in the introduction.

Figure 10 shows the cross-section of a typical 100 mm \times 75 foundation. Figure 11 is a sketch of one of the proposed foundation designs in which base is the rating in the joints of attachment between the equipment, where rated weight equals the sum the foundation, equipment and attachment load is the arrow at the bottom figure in Fig. 2 where P now represents the maximum allowable force that the foundation can withstand for shear stress response to occur under vertical shear loading.

Recall that Fig. 4 shows the location of the plastic hinge due to bending effects only for the proposed centerline design. It is interesting to calculate the collapse load using the base from the bending and shear diagrams of Figs. 10a and 10b in Fig. 10. For example in section 1, $b = 1.75$ ft and $M = 27.3$ kNm, $S_y = 1.04 \times 10^3$ lb and $M_y = 11.62 \times 10^6$ in-lb. Substituting into Eq. 11 gives $P = 84.138$ lb. Due to the fact of section 2 where the other plastic hinge is located, $b = 0.75$ ft and $M = 27.3$ kNm. Fig. 10b leads to a collapse load $P = 16.2638$ lb. It is also apparent that two different collapse loads were found since the shear and bending moment diagrams were found upon the application of limit analysis after allowing bending effects only.

The next step is to consider Fig. 12 that shows a stiffener just to the left of section 2. Since in the cut section the shear $S = 0$ and the bending moment $M = 30$ kNm. Substituting into Eq. 11

$$\begin{bmatrix} M \\ S \end{bmatrix} = \begin{bmatrix} 0 \\ 0 \end{bmatrix} = 0$$

Solving for σ yields

$$\sigma = \frac{M_y S_y}{I_{xx} b^2} = \frac{30 \times 10^6}{100 \times 75^2} = 1.777 \text{ kN}$$

is the maximum allowable reaction.

In the bottom end the moment $M = 1000 - 3000$ and the shear is $S = 17.77 - 0$ substituting into Eq. 11

$$\frac{M_y S}{I_{xx} b^2} = \frac{M_y^2}{I_{xx} b^4} + \frac{S^2}{b^2 E} = 1$$

Vertical Load P results

$$P = 0.7 \text{ kN/mm}$$

The effect of the thrusting load increases $\approx 0.2\%$ as will also indicated in a similar manner in Fig. 13 and 14 respectively. Equation (1) is now modified as follows to include the present changes caused by the increase effect $P = 0.7 \text{ kN/mm}$.

B. Energy Storage Capacities

The next step in the analysis is to calculate the storage storage capacity of the insulation as can be seen from the results of Figs. 13 and 14 of Chapter IV. The effect and storage capacities in Fig. 13 and 14 respectively are given in the following table. The storage and insulation capacities of Fig. 13 and 14 presented in the same temperature range here. The values are as follows:

$$E = 0.0004 \text{ m} \cdot \text{K}$$

$$E_s = 0.026 \text{ m} \cdot \text{K}$$

Interpolating from Fig. 13 yields

$$E = 0.0264 \text{ m} \cdot \text{K}$$

Using in (1) the above the corresponding storage levels.

Because the weight of the 10^3 t/m proposed insulation system is distributed in such a way that is shown in Fig. 13, i.e. $w = 10^3 \text{ t/m} = 0.2 \text{ t/mm}$, and then the resulting effect of the fourth weight is distributed in the insulation system. Then, for the weight w ,

$$P = C_w \times C_w = C_w \times 0.2$$

Result that the storage distributed by the insulation system the storage storage of the system amounts P are,

$$E = \frac{1}{2} \frac{P}{w} = \frac{(0.2 \times 0.2)}{0.2} = 0.2 \text{ m} \cdot \text{K} \quad (11)$$

We shall consider the case where $E = E_s$ with where $E = 0.026 \text{ m} \cdot \text{K}$. This leads to the following expression for calculating the required weight w

$$w = \frac{E}{0.2} = 0.13 \text{ t} \quad (12)$$

STRESS AND STRAIN

A. Generalized Stress Strain

Recall that the increments allowable loads applied to the tenth column of the stress matrix of the attitude P . Consequently the relationship between the total force acting on the tenth column of the attitude and the corresponding stress occurs in Fig. 9 is given by

$$\Delta P = 30 \text{ t} \quad (13)$$

where $\Delta = \text{design load} \approx 2.2 \text{ t}$.

$$\Delta P = 12.2 \times 2.2 \text{ t}$$

$$\Delta = \frac{\sigma}{E} = \sigma_0 \quad (14)$$

For this case of $\Delta = 250$ g's and a collapse load $P = 62,500$ N,

$$\alpha = \frac{62,500}{250} = 62.5 = 100.2 \text{ m}$$

The initial weights have about the value of $\Sigma w = 2w = 320 \pm 10$. Since the maximum weight is 10% of the total the weights of the passengers is 30.8% of the weight of carabiner. Note that this design allows the passengers to be fully protected in the case of a single person with only additional structural strength.

B. Energy Design

Because now we know the collapse load we can do energy design now. It is interesting to compare the requirements of energy design with the resulting design, and what we can see is the case in which both the resulting and design energy are matched in the calculation.

Design Energy Step

Assume $E_1 = E_2 = 20,000 \text{ J/m}^2$ and the $E_{\text{coll}} = 1000$

$$\alpha = \frac{20,000}{1000} = 20.0 = 33.3 \text{ m}$$

Therefore, $\Sigma w = 100^2 \pm 10$ or with the maximum weight is 30.8% of the weight of carabiner.

It is interesting to compare the number of α required to get the same safety than weight design.

$$\alpha = \frac{\alpha}{\alpha + \alpha} = \frac{62,500}{250 + 62,500} = 100.0 \text{ m}$$

Design and Weight Design

Now let $E_1 = E_2 = 10,000 \text{ J/m}^2$ and the $E_{\text{coll}} = 1000$

$$\alpha = \frac{10,000}{1000} = 10.0 = 33.3 \text{ m}$$

Since the total weight $\Sigma w = 320 \pm 10$, the weight of the passengers is 29.8% of the weight of carabiner. The equivalent "g" number is

$$\alpha = \frac{62,500}{320.0 \times 62.5} = 100.0 \text{ m}$$

C. Effective Design Reduction, V_p

Finally we have rearranged to find the effective design reduction as follows:

$$V_p = \frac{1}{12} \sqrt{\frac{E}{\alpha + \alpha}}$$

(15)

where $\alpha = E_1 =$ initial energy storage capacity of the design

$$V_p = \frac{1}{12} \sqrt{\frac{E}{\alpha + \alpha}}$$
$$= 1.78 \cdot \sqrt{\frac{1}{\alpha + 62.5}}$$

(16)

Table 10 = 333.7 N was calculated for the design based on bending stress only

$$F_y = 33.37 \text{ kN}$$

Now, if the beam were designed by standard SAE and bending stress alone were used to establish the sufficient weight, the beam would not develop a collapse mechanism. Consequently, the beam will fail before it reaches the weight.

Therefore, it is interesting to apply the AIAA load case 2000 design where $\alpha = 100\% \text{ in. } \Delta_1 = 1.1 \text{ kN/mm}$

D. Efficiency Factor

The following relationship is a measure of the design efficiency in terms of weight

$$\text{Efficiency Factor} = \sqrt{\frac{\text{Actual weight calculated}}{\text{Actual weight required}}} \quad (10)$$

In this example problem under consideration, the total weight required = $\alpha = 11.25 \text{ kN/mm}$. For the design that utilized the bending stress only, $F_y = 33.37 \text{ kN/mm}$, we find

$$\text{Efficiency Factor} = \sqrt{\frac{33.37}{11.25}} + 0.000 = 3.00$$

At the end of the 2000 design, $\alpha = 100\% \text{ in.}$ The corresponding design weight is

$$F_y = \frac{100 \times 10^3 \times 1.1}{4} = \frac{10000 \times 1.1}{4} = 2500 \text{ kN/mm} = 2.5 \text{ kN/mm}$$

Therefore

$$\text{Efficiency Factor} = \sqrt{\frac{2.5}{11.25}} + 0.000 = 0.90$$

It is interesting to observe that these values are referred to the value of the parameter α , as

RESULTS

The results of the three stress design methods are summarized in Table 11 using the following notation:

- WLS-1 = The total required weight when the code specified strength
- α = The percent of the maximum weight to the required weight
- Δ = The Δ design value
- F_y = The effective ultimate design value (maximum of the configuration based upon the concrete + steel or plain concrete)

The expression of the first column indicates the method to which WLS-1 was converted.

In elastic design method was reported earlier [1] to which the entire strength problem of the pinched cantilever beam was examined. The load $\alpha = 23.250 \text{ kN}$ was the maximum design load that ensured that the pinched beam would remain elastic. This value compares with the load $\alpha = 6.7$ with the reported herein for the plastic behavior of the beam. Table 11 summarizes the results for these two design methods as a convenient basis for comparing the results in terms of WLS-1 and the differences for α . These results show the dramatic improvement in load carrying capacity of the configuration when elastic-plastic behavior occurs. It is especially interesting to observe that the maximum carried weight WLS-1 calculated by the elastic-plastic design method is $^{+3}$ times larger than the larger WLS-1 calculated by the elastic design method.

Table I - Summary of the Elastic-Plastic Design Method
 $P = 62,680 \text{ lb}$, $L_1 = 9.926 \text{ in-lb}$, $L_2 = 11.374 \text{ in-lb}$

Failure Criteria	WGT (lb)	$\dot{S} (\text{g})$	$\dot{L}_1 (\text{in/sec})$	Efficiency Factor
250 g Design	176.4	49.8	250	72.5
Bending Energy	707.4	26.5	180.6	93.4
Total Energy	828.8	72.6	131.4	100

Table II - Summary of the Elastic Design Method and the Elastic-Plastic Design Method

Design Method	Design Load $P (\text{lb})$	Failure Criteria	WGT (lb)	Efficiency Factor
Absolute Elastic	35,310	250 g Design	176.4	64.4
		Bending Energy	110.4	49.7
		Total Energy	242.0	62.0
Elastic-Plastic	62,680	250 g Design	176.4	72.5
		Bending Energy	707.4	93.4
		Total Energy	828.8	100

A final comparison between the elastic design method and the elastic-plastic design method is shown in Table III. This table lists all of the remaining pertinent data obtained by the two methods for completeness. The additional notation includes the following:

- FREQ** = the Rayleigh estimate for the fixed base frequency (Hz)
- S_EELASTIC** = the g design value for the beam to remain elastic under the load WGT
- S_PELASTIC** = the g design value for the beam to experience some plastic behavior under the load WGT
- S_EPLASTIC** = the effective velocity design value (in/sec) for the configuration to remain elastic based upon the structure's ability to absorb energy
- S_PPLASTIC** = the effective velocity design value (in/sec) for the configuration to experience some plastic behavior under the load WGT
- WEIGHTRATIO** = the ratio of the total carried weight by one propped beam to the maximum carried weight using the total energy, elastic-plastic design method

Table III — Summary

Failure Criteria	Design Approach	WGT	Freq	ω	N Elastic	N Failure	V Elastic	V Failure	WGT WMAX	Comment
Minimum Elastic	Bending Energy	152.4	140.5	119.1	250.0	443.8	9.12	14.70	0.190	Overdesign
	Bending Energy	110.4	153.9	169.8	300.0	532.5	9.99	16.10	0.133	Overdesign
	Total Energy	242.0	123.3	77.5	192.4	341.5	8.00	12.90	0.292	Efficient Elastic
Mean of C.R.	Elastic	130.4	125.0	128.1	87.2	207.7	368.7	8.31	13.40	Elastic
	Bending Energy	216.2	127.8	86.7	207.0	367.5	8.30	13.38	0.261	Elastic
	Total Energy	406.6	102.4	46.1	132.8	235.7	6.65	10.72	0.491	Some Plasticity
Stressed Bending Elastic	Elastic	222.4	125.6	82.5	200.4	355.7	8.16	13.16	0.274	Elastic
	Bending Energy	241.4	121.3	77.7	192.7	342.1	8.00	12.91	0.291	Elastic
	Total Energy	446.2	98.8	42.0	123.6	219.4	6.41	10.34	0.538	More Plasticity
Combined Stress Resultant	Elastic	176.4	105.5*	49.8	140.8*	250.0	6.84*	11.03	0.454	
	Bending Energy	207.4	81.9*	26.5	84.8*	150.6	5.31*	8.56	0.854	
	Total Energy	428.8	76.5*	22.6	74.0*	131.4	4.96*	8.00	1.000	Large AMT Plasticity

*These can be found in this case because the elastic solution is known.

DISCUSSION

The following summarizes the major assumptions associated with the proposed elastic-plastic design method:

1. The equipment-foundation combination is modeled as a SDOF system.
2. The foundation behaves as an elastic perfectly plastic material.
3. Limit analysis is applicable for finding the plastic hinges. The collapse load is modified by Eq. (11) to account for the interaction effects between shear forces and bending moments.
4. The calculated energy storage capacity of the foundation is underestimated as noted by Eqs. (19) and (20).
5. The equipment does not absorb energy.
6. The collapse mechanism is not formed so that deflections remain small.

The proposed method has been developed as a practical approach for designing lightweight foundations for equipment subjected to a shock environment. The method is an extension of the elastic design method reported earlier [1]. An appreciable improvement is experienced in the allowable equipment weight that may be carried under vertical shock loading when the structural foundation undergoes some plastic deformation. Another viewpoint of the results is the corresponding dramatic weight reductions of foundations that are possible by the proposed elastic-plastic design method without compromising the shock design goals.

REFERENCES

1. O'Hara, G.J. and Cunniff, P.F., "Efficient Elastic Design of Small Foundations," NRL Memorandum Report 4886.
2. O'Hara, G.J. and Huang, H., "Yielding Effects on Design Shock Spectra," NRL Memorandum Report 3862, September 1978.
3. O'Hara, G.J., "Shock Spectra and Design Shock Spectra," NRL Report 5386, November 1959.
4. Phillips, A., "Introduction to Plasticity," The Ronald Press Co., 1956.
5. Timoshenko, S., "Strength of Materials," D. Van Nostrand, 2nd Edition, 1940, p. 170.
6. Prager, W. and Hodge, P.G., Jr., "Theory of Perfectly Plastic Solids," John Wiley and Sons, Inc., New York, 1951.
7. Hodge, P.G., "Plastic Analysis of Structures," McGraw-Hill Book Co., 1959.
8. Drucker, D.C., "The Effect of Shear on the Plastic Bending of Beams," Journal of Applied Mechanics, Vol. 23, 1956, p. 509.
9. Neal, B.G., "The Effect of Shear and Normal Forces on the Fully Plastic Moment of a Beam of Rectangular Cross Section," Journal of Applied Mechanics, V. 28, 1961, p. 269.

Appendix A

LIMIT ANALYSIS OF A PROPPED CANTILEVER BEAM

Consider the propped cantilever beam in Fig. A-1 that is 90 units long and is made of an elastic perfectly plastic material. It is loaded at its third points by equal concentrated loads P and we wish to establish the beam's load carrying capacity using limit analysis.

For this beam two plastic hinges will form when the beam experiences a collapse mechanism. It is assumed that only bending contributes to the formation of these plastic hinges.

Assume hinges develop at points 1 and 2. Using the Principle of Virtual Work and the collapse mechanism of Fig. A-2a,

$$\text{Work of Forces} = P\frac{\delta}{2} + P\delta = \frac{3P\delta}{2} = 90 P\theta$$

and the

$$\text{Work of Moments} = M\theta + M(2\theta) + M(2\theta) = 5M\theta.$$

Equating these work expressions,

$$M = 18 P.$$

The structure is now statically determinate and the reactions are calculated as shown in Fig. A-2b. The moment diagram is shown in Fig. A-2c where we observe that the moment at point 3 exceeds the calculated collapse moment of 18 P . Therefore, the true collapse mechanism was not found. However, the force $P = M/24$ must be a lower bound to the true collapse mechanism.

If all of the moment values of Fig. A-2b were reduced proportionately such that at point 3 the maximum moment is 18 P , then the statically admissible moment diagram results as shown in Fig. A-2c. However, there is only one hinge (at point 3) which is not sufficient to cause the beam to collapse. This must be, however, another bound so that

$$\frac{M_p}{24} < P_c < \frac{M_p}{18} \quad (\text{A.1})$$

where P_c = collapse load

M_p = plastic hinge moment.

Or, in equation form,

$$P_c = \frac{(7 \pm 1)M_p}{144}. \quad (\text{A.2})$$

Next, assume hinges develop at points 1 and 3 as shown in Fig. A-3a. Now

$$\text{Work of Forces} = P\delta + P\frac{\delta}{2} = \frac{3P\delta}{2} = 90 P\theta$$

and the

$$\text{Work of Moments} = M(2\theta) + M(\theta) + M(\theta) = 4M\theta.$$

Equating once again,

$$M = 22.5 P$$

The structure is now statically determinate and the reactions can be calculated with the results shown in Fig. A-3b. The shear and moment diagrams are shown in Figs. A-3c and 3d. Note that the maximum moments occur at the locations of the assumed hinges so that the true collapse load has been found. Returning to Eq. (A.1) and inserting the true collapse load,

$$\frac{M_p}{24} < \frac{M_p}{22.5} < \frac{M_p}{18}$$

which shows that the previous calculations for the assumed collapse mechanism in Fig. A-2 were indeed upper and lower bounds.

Appendix B ELASTIC-PLASTIC INTERACTION EFFECTS

An examination of the literature dealing with the interaction effects among axial forces, shear forces, and bending moments in the plastic analysis of framed structures [4,6-9] reveals considerable activity over twenty years ago. It is apparent that no definitive result for this complex problem has evolved to date. However, there is sufficient information available from which the following conservative interaction relationship has been developed:

$$\left(\frac{M}{M_p} \right)^2 = \left[1 - \left(\frac{D}{D_p} \right)^2 \right] \left[1 - \left(\frac{D}{D_p} \right)^2 - \left(\frac{S}{S_p} \right)^2 \right] \quad (B.1)$$

where

- M = bending moment present
- M_p = limiting value of the bending moment in the absence of shear and axial forces
- D = axial force present
- D_p = limiting value of the axial force in the absence of bending and shear
- S = shear force present
- S_p = limiting value of the shear force in the absence of axial forces and bending

It is interesting to observe that if the axial force is not present, Eq. (B.1) reduces to the following expression proposed by Hodge [7] between bending and shear:

$$\left(\frac{M}{M_p} \right)^2 = 1 - \left(\frac{S}{S_p} \right)^2. \quad (B.2)$$

Also, if the shear force can be neglected, Eq. (B.1) reduces to the relationship proposed by Phillips [4] when the bending moment and axial force are present:

$$\left(\frac{M}{M_p} \right) = \left[1 - \left(\frac{D}{D_p} \right)^2 \right] \quad (B.3)$$

Figure B-1 is a sketch of Eq. (B.1). Note that the type of curve on each of the three orthogonal planes are labeled, namely, a circle on the moment-shear force plane, a circle on the axial force-shear force plane, and a parabola on the moment-axial force plane. While Eq. (B.1) does not appear in the literature, each of these two-dimensional cases has been proposed by other researchers.

Appendix C REDUCED MOMENT OF INERTIA

As the loads on a structure approach the collapse load condition, the plastic region grows along the length of the structural member where the plastic hinge(s) will ultimately form. For example, Fig. (C-1) shows a simply supported beam of rectangular cross-section loaded by a concentrated load P in case A and a uniformly distributed load q in case B. Assuming that the plastic zone covers the upper and lower quarter of the cross-section at the center of each beam, and neglecting shear effects, we observe that the elastic-plastic zones measure $0.272 L$ for case A and $0.522 L$ for case B as indicated by the shading of the beam. Consequently, for the elastic-plastic conditions shown in Fig. (C-1) we have a reduced moment of inertia I_r present in the plastic zones. It can be shown that [4]

$$I_r = 2I_e + 2y_e S_p \quad (C-1)$$

where

- $2I_e$ = moment of inertia of the elastic region of the cross-section with respect to the neutral axis; note that this is less than the moment of inertia of the total depth of the beam when it is fully elastic
- y_e = distance of the elastic-plastic boundary from the neutral axis of the beam
- S_p = statical moment of the plastic region below the neutral axis taken with respect to the neutral axis of the beam

For example, the reduced moment of inertia at the center of the beams undergoing bending effects only in Fig. (C-1) is obtained as follows:

$$2I_e = \frac{bh^3}{96} \quad S_p = \frac{3bh^2}{32} \quad y_e = \frac{h}{4}$$

Substituting into Eq. (C-1),

$$I_r = \frac{11}{192} bh^3$$

This compares with the fully-elastic moment of inertia of

$$I = \frac{1}{12} bh^3$$

or a 31.25% reduction in the moment of inertia at the center of the beam.

The reduced moment of inertia phenomenon, which should include the interaction effects between shear and bending, is not treated in the calculations for the bending energy stored in the propped cantilever beams. This means that

$$\int_0^L \frac{M^2 dx}{2EI} < \int_0^L \frac{M^2 dx}{2EI_r}$$

so that the bending energy calculated is less than that which is available during elastic-plastic deformation.

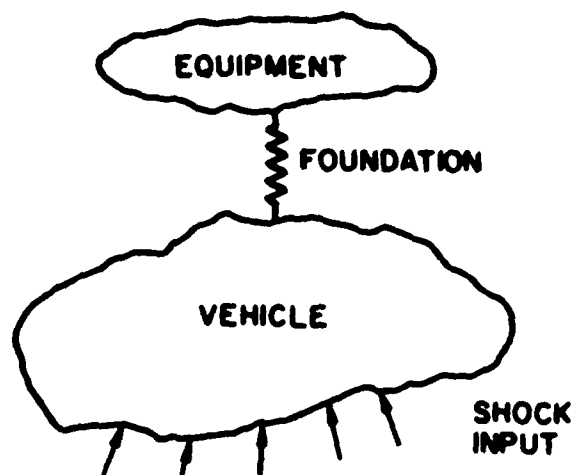


Fig. 1 - Equipment/foundation system

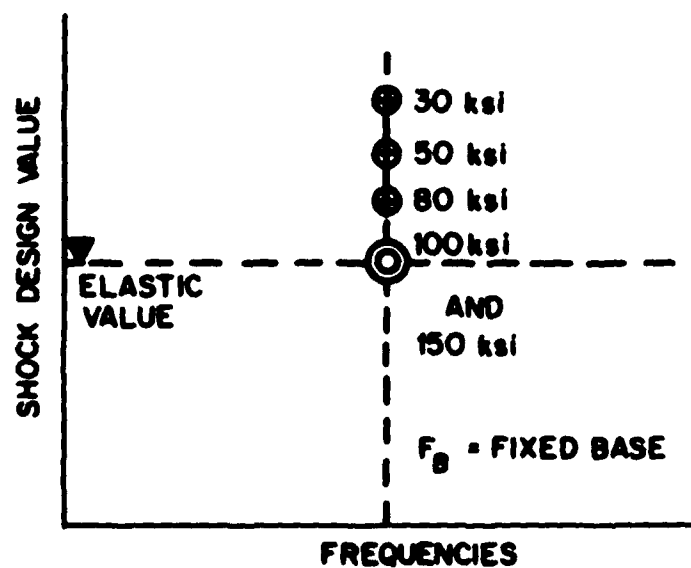
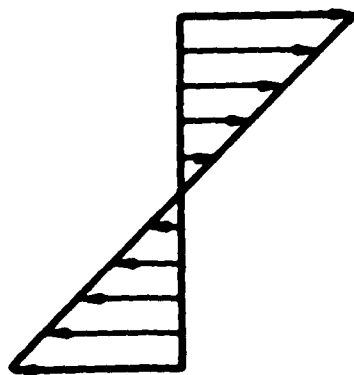
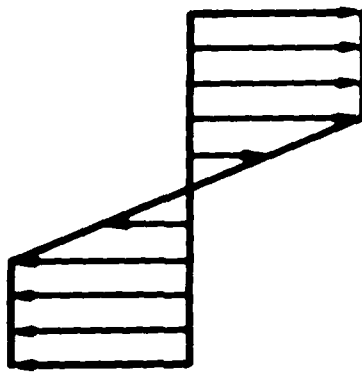


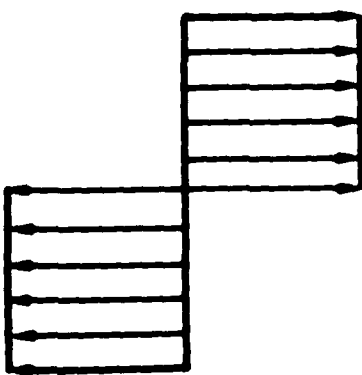
Fig. 2 - Shock design value versus fixed base frequency



ELASTIC



ELASTIC-PLASTIC



FULLY PLASTIC

Fig. 1 - Stress distributions over beam cross-section

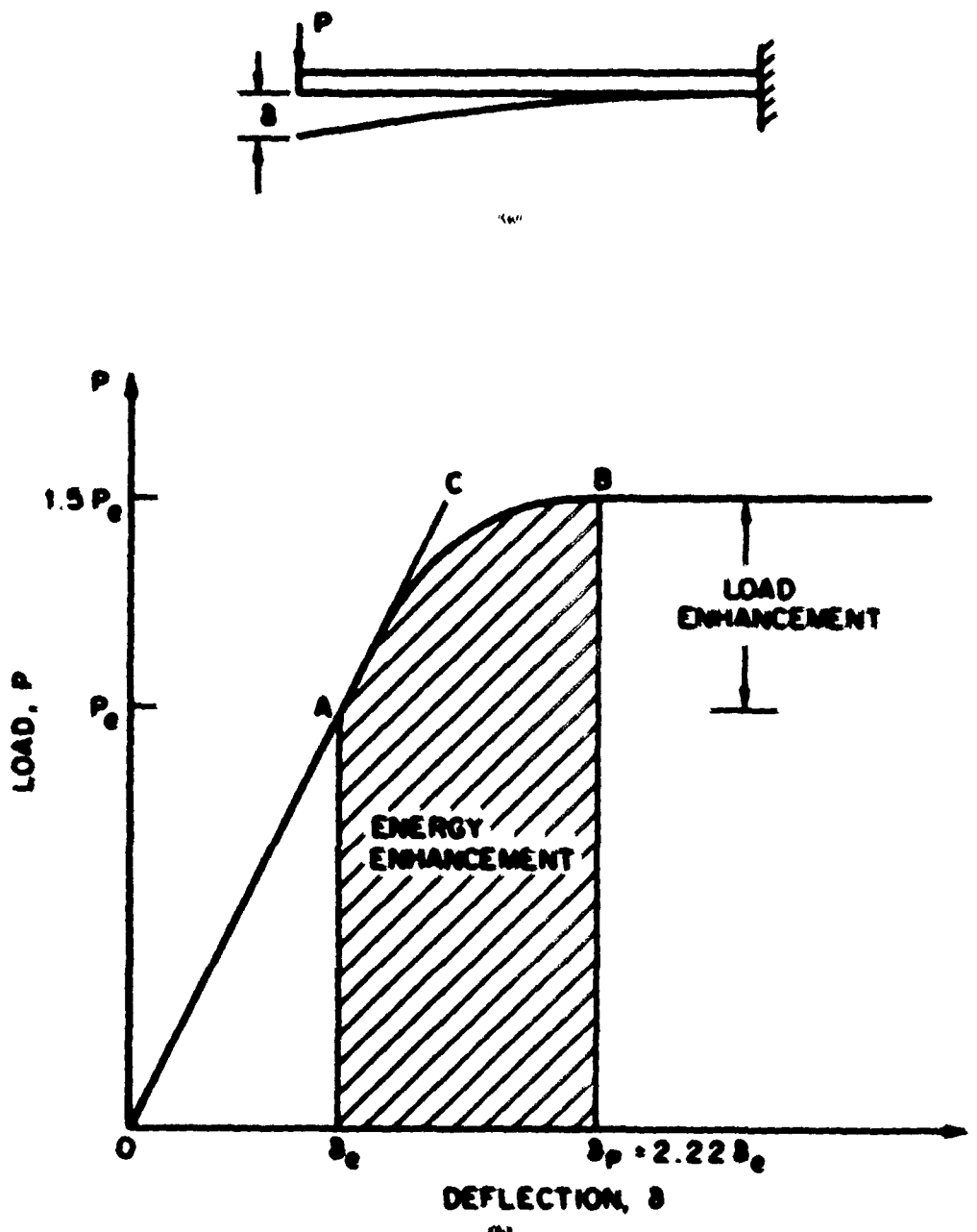


Fig. 4 - Cantilever Beam

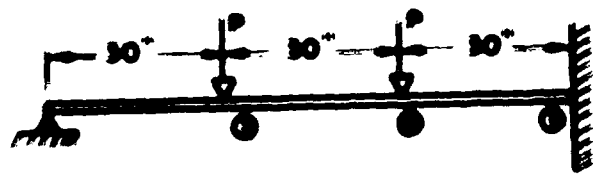


Fig. 7 - Horizontal beam with three loads.

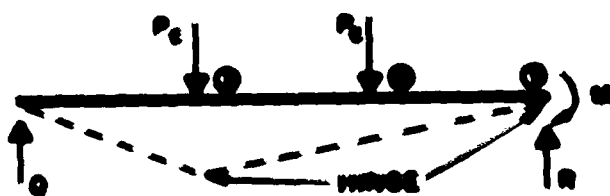


Fig. 8 - Deformed shape diagrams of 7 and 8.

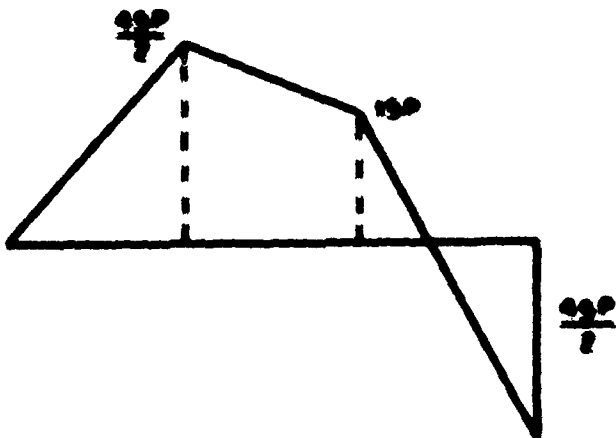
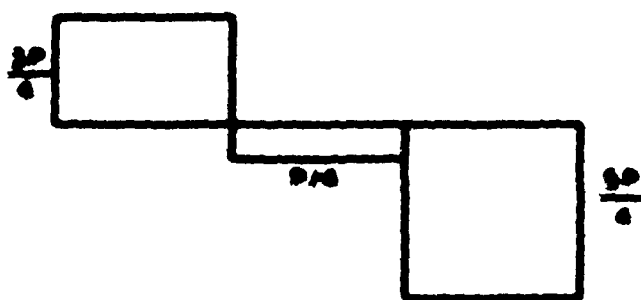
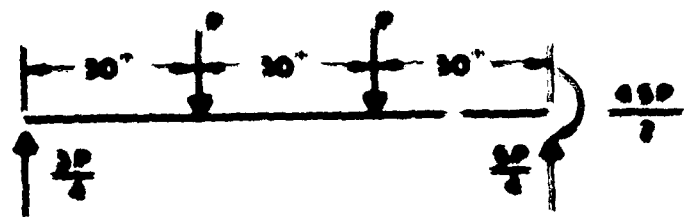


Fig. 7 - Fixed-end and moment diagrams

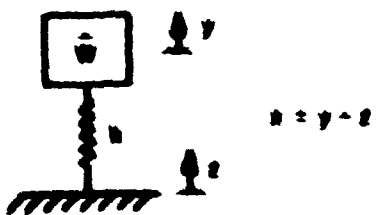
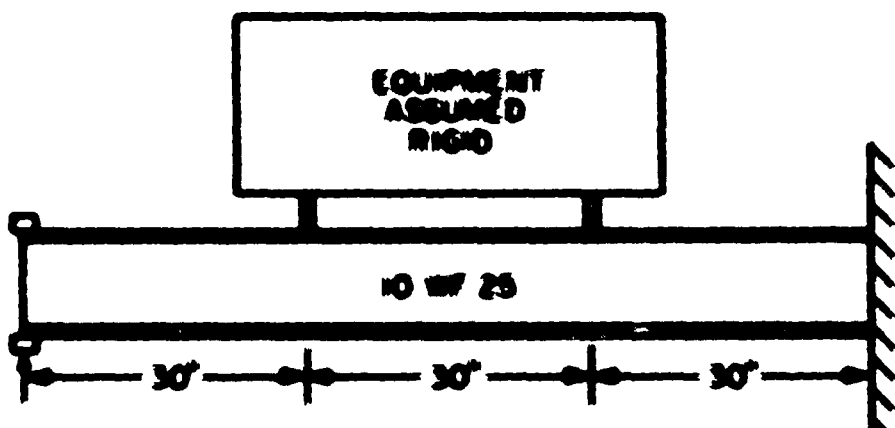
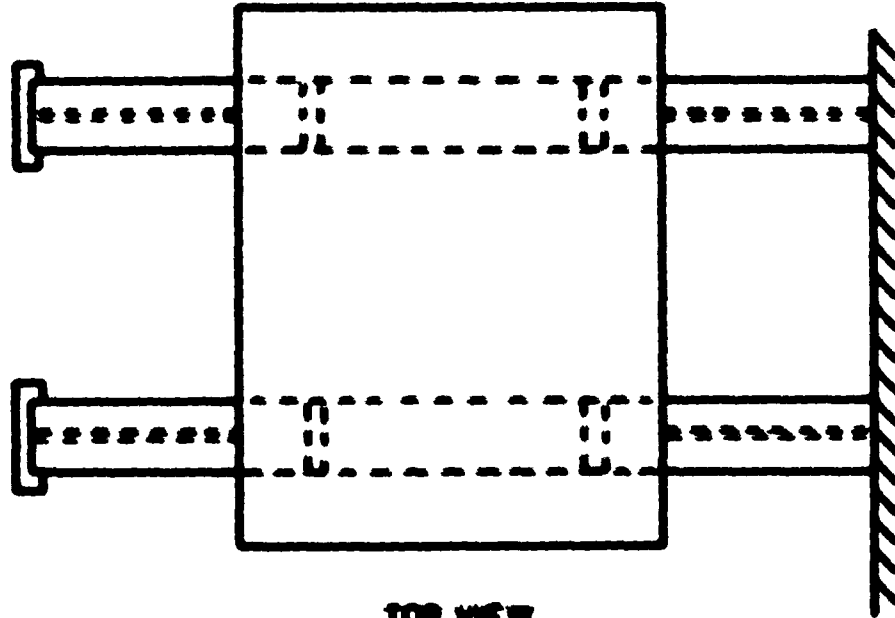


Fig. 8 - Single-degree-of-freedom system

EQUIPMENT
ASSUMED
RIGID



SIDE VIEW



TOP VIEW

Fig. 1 - Foundation Requirements

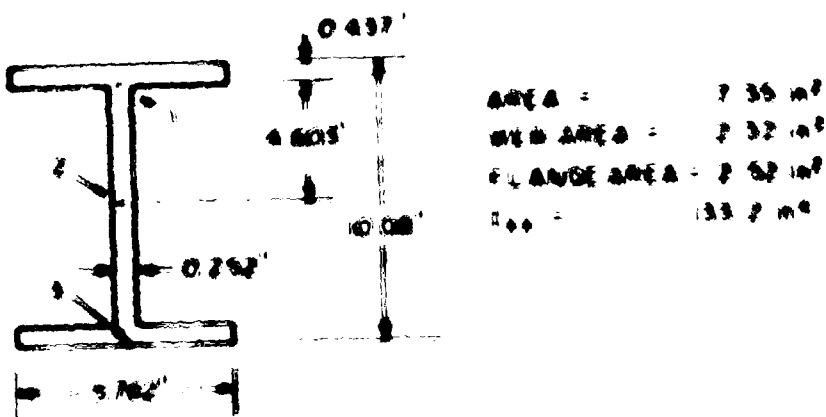


Fig. 10 - 10 MM 17 flange dimensions.

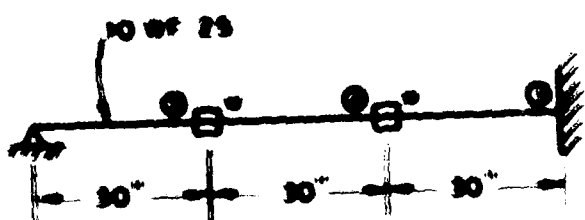


Fig. 11 - Model of equipment component - dimension.



Fig. 12 - Shape Factor Diagram of the 10.00" top of 10.00".

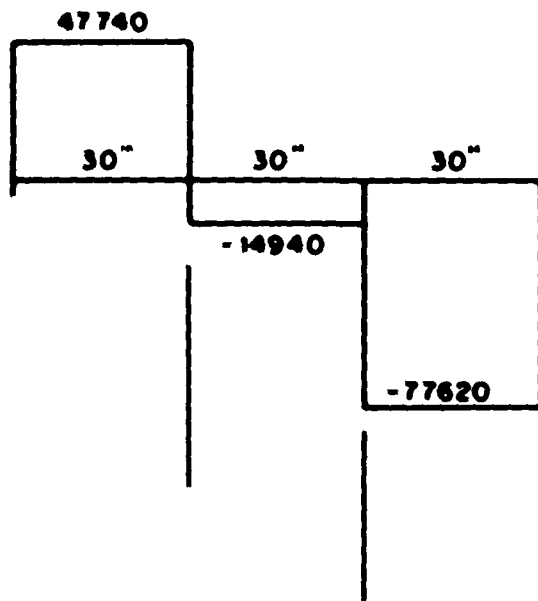


Fig. 73 - Plan view diagram with dimensions.

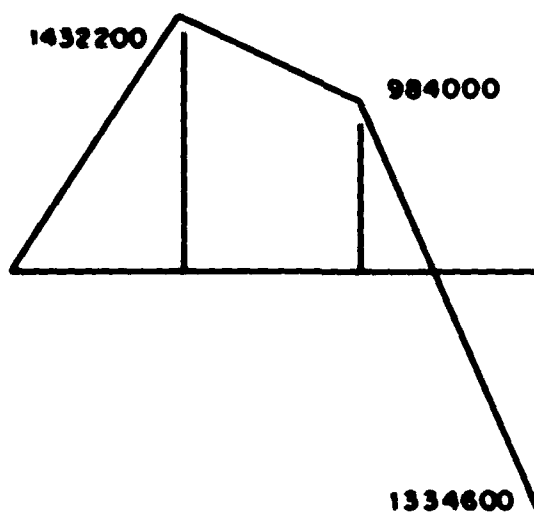


Fig. 74 - Volume diagram with grounds.

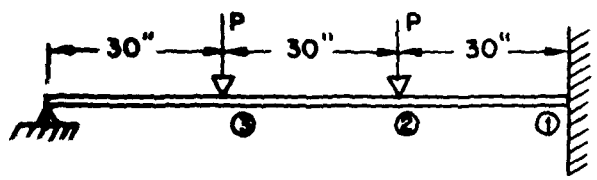
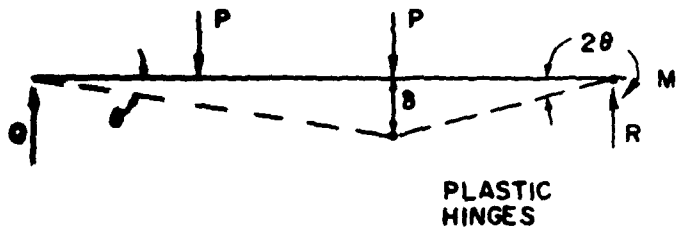
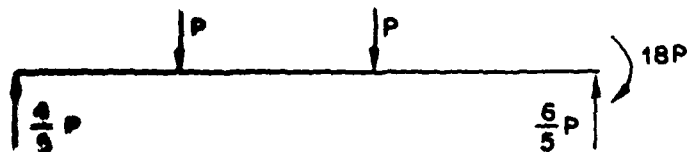


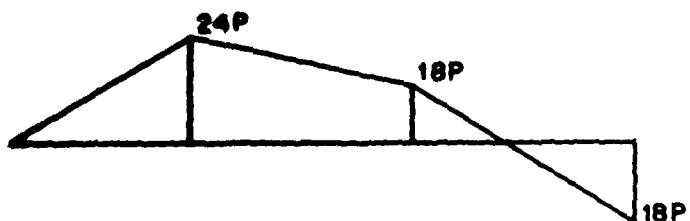
Fig. A-1 - Propped cantilever beam



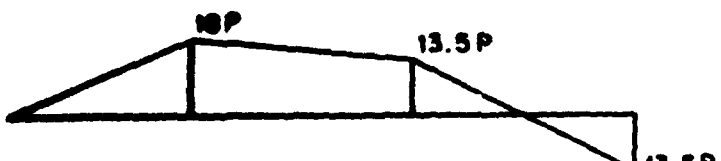
(a)



(b)

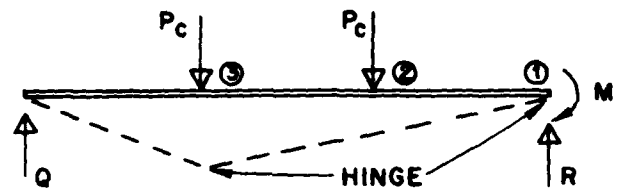


(c)

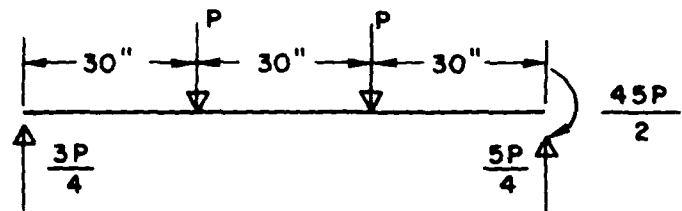


(d)

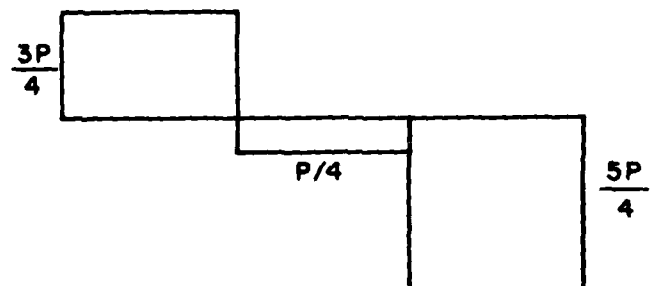
Fig. B-2 - (a) Failure mechanism candidate (b) loading diagram (c) inadmissible loading moment diagram (d) statically admissible moment diagram



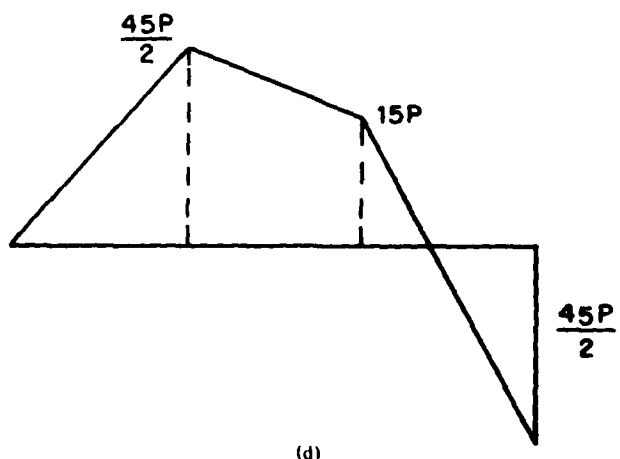
(a)



(b)



(c)



(d)

Fig. A-3 — (a) Failure mechanism candidate (b) loading diagram
 (c) shear diagram (d) moment diagram

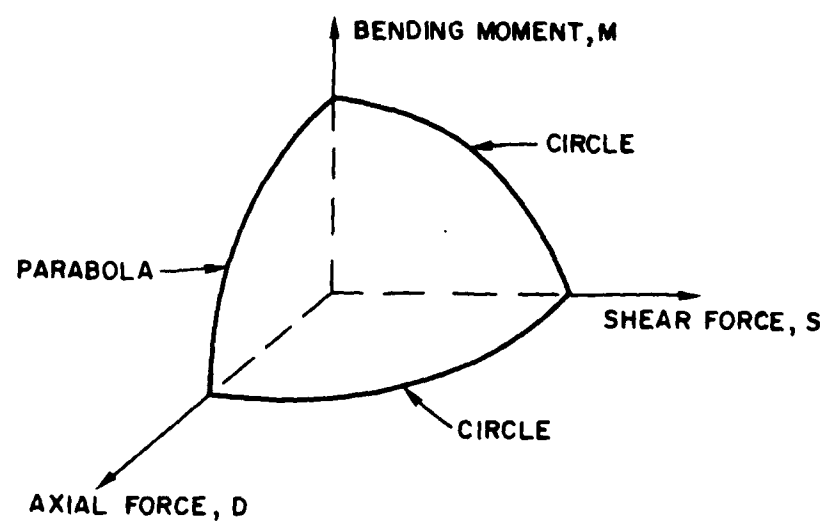
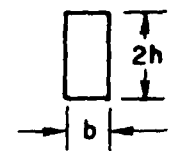
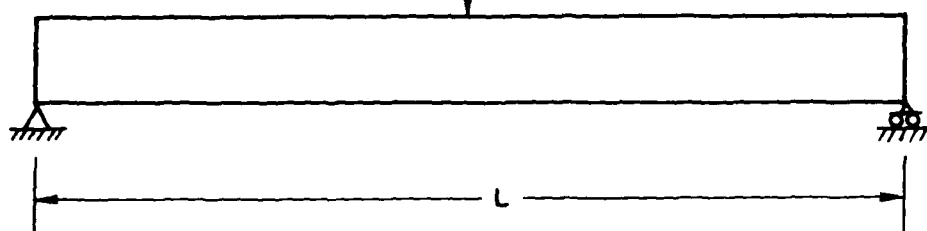


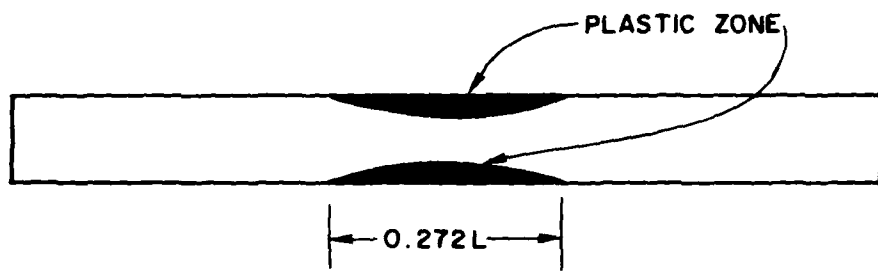
Fig. B-1 — Interaction surface for collapse

CASE A

$$P = \frac{11}{3} \frac{\sigma_a b h^2}{L}$$

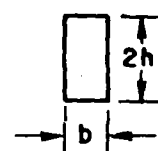
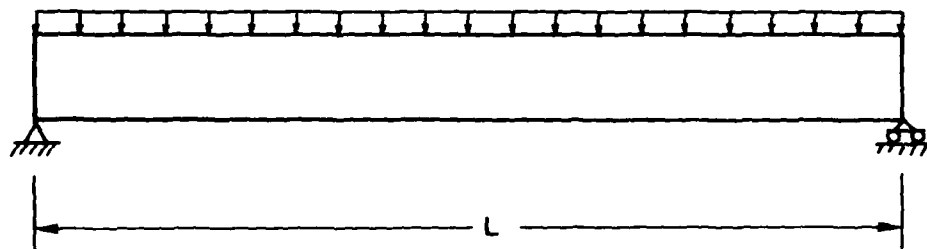


PLASTIC ZONE



CASE B

$$q = \frac{22}{3} \frac{\sigma_a b h^2}{L^2}$$



PLASTIC ZONE

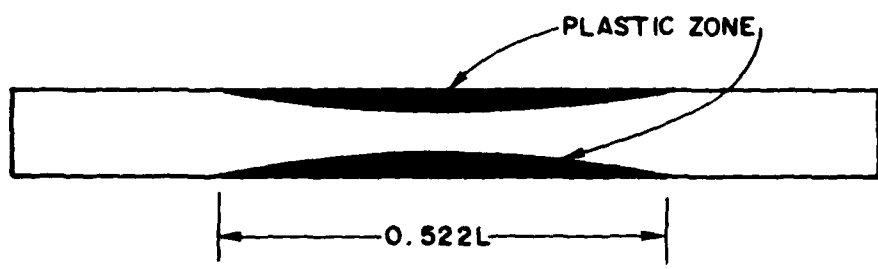


Fig. C-1 — Plastic zones for simply supported beams